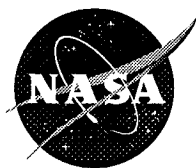


NASA/TM—1998-208484

AIAA-98-3288



Feasibility Assessment of Thermal Barrier Seals for Extreme Transient Temperatures

Bruce M. Steinetz
Lewis Research Center, Cleveland, Ohio

Patrick H. Dunlap, Jr.
Modern Technologies, Corp., Middleburg Heights, Ohio

Prepared for the
34th Joint Propulsion Conference
cosponsored by AIAA, ASME, SAE, and ASEE
Cleveland, Ohio, July 12-15, 1998

National Aeronautics and
Space Administration

Lewis Research Center

July 1998

Acknowledgments

The authors gratefully acknowledge Doug Frost's and Peter Totman's (Thiokol) thermal barrier seal "char" motor test results; Bruce Bond's (Albany-Techniweave) assistance in fabricating the seals; and Tom Doeberling's (NASA) assistance in test support.

Trade names or manufacturers' names are used in this report for identification only. This usage does not constitute an official endorsement, either expressed or implied, by the National Aeronautics and Space Administration.

Available from

NASA Center for Aerospace Information
7121 Standard Drive
Hanover, MD 21076
Price Code: A03

National Technical Information Service
5287 Port Royal Road
Springfield, VA 22100
Price Code: A03

FEASIBILITY ASSESSMENT OF THERMAL BARRIER SEALS FOR EXTREME TRANSIENT TEMPERATURES

Bruce M. Steinetz*

National Aeronautics and Space Administration
Lewis Research Center
Cleveland, Ohio 44135

Patrick H. Dunlap, Jr.†

Modern Technologies Corporation
Middleburg Heights, Ohio 44130

Abstract

Assembly joints of modern solid rocket motor cases are generally sealed using conventional O-ring seals. The 5500 °F combustion gases produced by rocket motors are kept a safe distance away from the seals by thick layers of phenolic insulation. Special compounds are used to fill insulation gaps leading up to the seals to prevent a direct flowpath to them. Design criteria require that the seals should not experience torching or charring during operation, or their sealing ability would be compromised. On limited occasions, NASA has observed charring of the primary O-rings of the Space Shuttle solid rocket nozzle assembly joints due to parasitic leakage paths opening up in the gap-fill compounds during rocket operation. NASA is investigating different approaches for preventing torching or charring of the primary O-rings. One approach is to implement a braided rope seal upstream of the primary O-ring to serve as a thermal barrier that prevents the hot gases from impinging on the O-ring seals.

This paper presents flow, resiliency, and thermal resistance for several types of NASA rope seals braided out of carbon fibers. Burn tests were performed to determine the time to burn through each of the seals when exposed to the flame of an oxyacetylene torch (5500 °F), representative of the 5500 °F solid rocket motor combustion temperatures. Rope seals braided out of carbon fibers endured the flame for over six minutes, three times longer than the solid rocket motor burn time. Room and high temperature flow tests are presented for the carbon seals for different amounts of linear compression. Room temperature compression tests were performed to assess seal resiliency and unit preloads as a function of compression. The thermal barrier seal was tested in a subscale "char" motor test in which the

seal sealed an intentional defect in the gap insulation. Temperature measurements indicated that the seal blocked 2500 °F combustion gases on the upstream side with very little temperature rise on the downstream side.

Introduction

The need for high temperature (1500-2000 °F) compliant seals in increasingly demanding gas turbine engine designs led to the development of rope seals braided out of emerging ceramic fibers and superalloy wires. Previous seal research yielded several braided rope seal designs that demonstrated the ability to both seal and serve as compliant mounts under aggressive temperature and pressure requirements.^{1,2} These seals have low leakage, exhibit resiliency with cycling to maintain a good seal, resist scrubbing damage, seal complex geometries, and support structural loads. Steinetz et al.¹ and Steinetz and Adams² studied both all-ceramic and hybrid designs that were applied in industrial tube seal and high or low pressure turbine vane seal applications. The material systems used in these braided rope seal designs function very well at the temperatures experienced in advanced gas turbine engines. However, as revealed later in this study, these seals do not last for more than a few seconds when subjected to the extremely hot 5500 °F combustion gases that are found in rocket applications. Thus, other materials had to be considered to advance the braided rope seal design into a thermal barrier seal for use at extreme transient temperatures.

Solid rockets, including the Space Shuttle reusable solid rocket motor (RSRM), have assembly joints that are usually sealed by conventional O-ring type seals. These seals are shielded from the 5500 °F combustion gases by

*Senior Research Engineer, Mechanical Components Branch,
Member AIAA.

†Research Engineer.

Copyright © by the American Institute of Aeronautics and Astronautics, Inc. No copyright is asserted in the United States under Title 17, U.S. Code. The U.S. Government has a royalty-free license to exercise all rights under the copyright claimed herein for Governmental Purposes. All other rights are reserved by the copyright owner.

thick layers of phenolic insulation and by special compounds that fill gaps in this insulation. Normally, these two stages of protection are enough to prevent a direct flow of the 900 psi hot gases to the seals. Occasionally, though, seals have experienced charring due to parasitic leakage paths that open up in the gap-filling compounds during rocket operation, requiring another level of protection for the primary O-rings. Inspection during disassembly of Space Shuttle solid rocket motor nozzle joints from RSRM-44 and RSRM-45 revealed O-ring erosion of joint 3 primary O-ring seals³ (Figure 1). NASA and rocket manufacturer Thiokol are investigating nozzle joint design enhancements, such as the proposed thermal barrier seal (Figure 1a), to prevent hot combustion gases from reaching the Viton primary O-rings. Nozzle joints 1 through 5 in Figure 1 are currently being studied. The braided carbon thermal barrier seal being developed at NASA Lewis is a leading candidate based on the results presented herein.

The thermal barrier seal has unique requirements for the Shuttle solid rocket motor joints, including the following, amongst others:

1. Sustain extreme temperatures (2500-5500 °F) during solid rocket motor burn (2 minutes and 4 seconds) without loss of integrity.
2. Block 900 psi hot flow gases from impinging on primary O-rings to prevent O-ring char or erosion.
3. Exhibit some permeability to allow pressure check of primary/secondary O-ring system without any "false-positives" of the primary O-ring seal.
4. Exhibit adequate resiliency/springback to accommodate limited (0.003-0.005 in.) joint movement/separation and to seal manufacturing tolerances in these large nozzle segments (diameter range 4.8 ft. to 7.3 ft.).

Over the past few decades, carbon fibers have been used in a wide variety of applications in aerospace because of their excellent combination of thermal and mechanical properties. Among heat-resistant fibers, carbon fibers have been widely used because of their relatively high heat conduction, low linear expansion coefficient, and high corrosion and thermal stability as well as their high strength and low density.⁴ Though braided carbon seals have been used for nuclear applications, there are no known uses of this type of seal for solid rocket applications. Although carbon fibers oxidize and lose mass over periods of several hours at temperatures above 600 to 900 °F (depending on the type of fiber),^{5,6,7} they are able to withstand very high temperatures for short periods of time.

The main objective of the current study was to evaluate the thermal resistance of braided rope seals made of different materials, including carbon, when exposed to

extremely high temperature gases. The seals that endured these gases the longest were then subjected to flow and compression tests. Subscale rocket "char" motor tests were performed to assess the thermal barrier seal's heat resistance under actual rocket conditions.

Test Apparatus and Procedures

Seal Specimens

Several types of seals were examined for each different series of tests. Carbon, phenolic, hybrid, and all-ceramic braided rope seals were all subjected to burn tests. Buna-N and Viton rubber seals and a 1/8 inch diameter stainless steel rod were also burn tested as references to compare to the braided rope seals. Table 1 summarizes the relevant architecture parameters for the braided rope seals that were tested. All braided rope seals were composed of a dense uniaxial core of fibers overbraided with a single- or multi-layer sheath.

The Carbon-1 design had five sheath layers and a 0.114 in. diameter, while the Carbon-2 seals had ten sheath layers and a 0.125 in. diameter. Both the Carbon-3 and Carbon-4 designs had five sheath layers. However, Carbon-3 seals had a 0.200 in. diameter, and Carbon-4 seals had a 0.194 in. diameter. Carbon-4 seals had 4.4×10^{-4} in. (11 μm) pitch-based Amoco P25 fibers in their cores to evaluate core fiber diameter effects on performance, while the core fibers of all the other carbon braided rope seals were 2.76×10^{-4} in. (6.9 μm) PAN-based Grafil type 34-700 fibers. PAN-based Thornel T-300 carbon fibers with a 2.8×10^{-4} in. (7 μm) diameter were used in the sheaths of all the carbon seals. The phenolic seals had a core composed of Kynol KFY-0204-1 fibers with diameters of 6.0×10^{-4} in. (15 μm) and a four-layer sheath of 6.0×10^{-4} in. (15 μm) Kynol KY-02 fibers. Hybrid and all-ceramic braided seal construction details are presented in Table I.

Seal Characterization

To assess seal architecture characteristics, samples of each carbon fiber braided rope seal design were examined using a photographic stereomicroscope. Two cross sections of each type of seal about 1/16 in. thick were prepared and examined under the microscope. Photographs were taken of each side of the specimen at 30X for the 0.20 in. diameter seals or 40X for the 1/8 in. diameter seals so that four cross section photos were examined for each type of seal. None of the core areas were completely round, so the dimensions of the core were measured using vernier calipers. These dimensions were then used to calculate the area of the core in the cross section. For each area, an equivalent core diameter was calculated as if the core was circular. The core diameters were then used along with the

overall seal diameter for each seal design to calculate the sheath thickness using the following relationship:

$$\text{Seal Diameter} = \text{Core Diameter} + 2(\text{Sheath Thickness})$$

These values were then averaged from the four photographs to obtain an equivalent core diameter and sheath thickness for each type of carbon seal.

Overall seal density measurements were also made for each carbon seal. Three 4 in. specimens of each type of seal were prepared and weighed using a precision electronic balance. The length and diameter of each specimen were measured using vernier calipers. The overall seal density of each specimen was then calculated by dividing the weight of the specimen by its volume. The overall seal density of each type of seal was then calculated by averaging the values obtained from the three specimens.

Burn Tests

A simple screening test was developed to evaluate thermal barrier seal burn resistance under simulated rocket motor combustion temperatures (5500 °F) by aiming a "neutral" flame of an oxyacetylene welding torch at the center section of a four inch seal specimen. In these tests, the amount of time required to completely cut through the specimen was measured. Time for cut-through was measured from the instant the flame touched the specimen until the specimen was completely cut into two separate pieces. These tests were performed using two different setups. The first setup mainly screened different types of seal materials. One end of the four inch seal sample was held in a clamp, and the remainder of the seal hung vertically below the clamp. The oxyacetylene torch was adjusted to a neutral flame, and the flame was manually applied to the center section of the seal with the nozzle exit about one inch away from the specimen. The time to burn through the seal was recorded from the instant the flame hit the seal until the seal was completely cut in half and the lower half of the seal fell to the floor. Several different seal materials were tested including: all-ceramic, hybrid, phenolic, and carbon seals. All specimens had 1/8 in. diameters. Rubber O-rings made of Buna-N and Viton, and a 1/8 in. diameter stainless steel rod were also tested for comparison purposes. This method was not well-controlled as the application of the flame to the seal was subject to the torch operator's ability to hold the torch steady and in the same position from test to test. Thus, a more repeatable, consistent method of performing these tests was designed.

In this second approach, two seal specimens, the test seal and a flame calibration seal, were clamped in place in the fixture so that the seal surface closest to the torch was

0.30 in (7.5 mm) from the stationary nozzle (Figure 2). The carriage that held the clamps was capable of sliding along a machined groove so that either seal could be positioned in front of the oxyacetylene torch at the same prescribed distance. The torch was placed in between the two seals and ignited. The first time that the torch was lit for a given series of tests a neutral flame⁸ was formed by adjusting the valves on the torch handle. The flame calibration seal was then slid into the flame to check that the tip of the inner cone of the flame (the hottest part of the flame)⁸ was 0.08 in. (2 mm) from the edge of the seal specimens. Theoretical calculations based on the chemical reactions that occur as the flame burns estimate the temperature at the tip of the inner cone to be about 5500 °F.⁹ The test seal was then slid into the flame, and the amount of time to burn through the seal was recorded. End-stop clamps were positioned on the fixture at either end of the groove to position the seals directly in the center of the flame as the carriage moved from one end of the groove to the other. Between tests the gas supply was shut off at the bottles so as not to disturb the sensitive oxygen/acetylene mixture that was regulated at the torch. This ensured that the same mix of oxygen and acetylene was used to burn through each specimen and that the flame was consistent from test to test. After a burned test specimen was removed from the fixture, a new specimen was clamped in place 0.30 in. from the nozzle, and the torch was relit between the specimens. Because the valves on the torch had already been adjusted for a neutral flame, no additional adjustments were needed. However, the position of the flame was always verified using the flame calibration seal before sliding the test seal into the flame. Specimens of all four carbon fiber braided rope seal designs were tested using this fixture. The Carbon-1 and Carbon-2 designs had nominal diameters of 1/8 in., while the Carbon-3 and Carbon-4 seals had nominal 0.20 in. diameters. An additional design was also tested in which the last sheath layer was removed from a Carbon-2 seal. This seal only had nine sheath layers and was referred to as Carbon-2A.

Flow Tests

Flow tests were performed on the seals in a high temperature flow and durability test rig shown schematically in Figure 3. Seal specimen length was 8.00 ± 0.05 in., and the seals were mounted into a groove in the piston. The free ends of the seals were joined together in the piston groove using a 1/4 in. lap joint. Preload was applied to the seals through a known interference fit between the seal and the cylinder inner diameter. To vary the amount of preload, the interference fit was modified by mounting different thicknesses of stainless steel shims behind the seal in the piston groove. Prior to flow testing, seal specimens were preworked or precompressed to minimize damage to the seals during the process of inserting

the piston/seal assembly into the cylinder. Details of the preworking procedure are described in depth by Steinetz and Adams.² After being preworked, the piston/seal assembly was inserted into the cylinder for testing. During flow testing, hot pressurized air entered at the base of the cylinder and flowed to the test seal that sealed the annulus created by the cylinder and piston walls. A radial gap of 0.007 in. between the piston and the cylinder created this annulus. The durability of the rope seals at high temperatures was examined by subjecting them to scrub cycles in which the piston and seal were reciprocated in the cylinder. This movement simulated relative thermal growths between structures that the rope seals would be sealing. Movement of the piston within the cylinder was guided by preloaded precision linear bearings. The piston stroke for each cycle was 0.125 in., so for each cycle the seal sliding distance was 0.25 in.

The test rig is capable of operating at temperatures from room temperature to 1500 °F, pressures between 0 and 100 psig, and flows of 0 to 3.5 SCFM (standard cubic feet per minute). Other details of the high temperature flow and durability test rig including hardware, heating systems, measurement techniques and probe accuracy have been previously described in depth by Steinetz et al.¹ Seal flow data was recorded before scrubbing at temperatures of 70 and 500 °F and after scrubbing at 70, 500, and 900 °F. Seals were subjected to ten scrub cycles at 500 °F. No prescrubbing flow data was collected at 900 °F to minimize the amount of carbon fiber oxidation that occurred while the seal sat at that temperature during rig heat up. At each temperature, flow data was recorded at pressures of 2, 5, 10, 30, 60, 90, and 100 psid with the downstream pressure at ambient pressure. Primary and repeat flow tests were performed on the 1/8 in. diameter Carbon-1 and Carbon-2 designs for linear seal compressions of 0.025 and 0.031 in. (20 and 25% linear compression). For the 0.20 in. diameter Carbon-3 and Carbon-4 designs, only primary flow tests were performed at a compression of 0.040 in. (20% linear compression).

During data collection, special care was taken to monitor the relative temperatures of the piston and cylinder. The cylinder outer wall temperature and the inner wall temperature of the hollow piston were monitored. Flow data was only collected when the temperature difference between these surfaces was less than 40 °F. Under operating conditions, a forty degree temperature difference results in less than a 0.0003 in. change in the sealed gap at 900 °F.

A thermal growth differential exists between the carbon-based seal and the Inconel X-750 superalloy piston. This is especially enhanced by the fact that carbon fibers have a negative coefficient of thermal expansion in the

longitudinal (e.g., circumferential) direction of $-0.3 \text{ PPM}/^\circ\text{F}$.¹⁰ Thus, at high temperatures the piston circumferentially outgrows the seal, and the seal ends move apart. To compensate for this phenomenon, the seal free ends were joined together as a lap joint to prevent a free flow path from forming (Figure 3). A lap joint of at least 1/4 in. was used to prevent the joint from opening and to mitigate the effects of 0.053 in. in relative piston-to-seal differential circumferential growth.

Compression Tests

Compression tests were performed to determine seal preload and resiliency behavior at room temperature using a precision linear slide compression test fixture shown schematically in Figure 4. A seal was loaded into a stationary grooved seal holder, and an opposing plate was compressed against the seal. The amount of compressive load on the seal was measured versus the amount of seal compression. Seal compression, or linear crush, was measured using a digital indicator that monitored the movement of the opposing plate relative to the stationary seal holder. A pressure sensitive film mounted on the opposing plate was used to determine the contact width of the seal as it was compressively loaded. The film develops under compressive loading so that the seal leaves a "footprint" after it has been crushed against the opposing plate. The loading characteristics of the pressure sensitive film were described in detail by Steinetz and Adams.² Average compressive load, or preload, was calculated by dividing the measured compressive force recorded during loading by the seal contact area left on the film.

As with the flow tests, stainless steel shims were placed in the groove behind the seal specimens so that different amounts of linear compression could be examined. The ends of the specimens were lightly glued to prevent the short seal lengths from unraveling. The seal specimens used for these tests were 1 1/2 in. in length, and the shims placed behind the seals were 1 in. long. This allowed the ends of the seal to hang over the ends of the shims. Isolating the glued ends of the specimens from the test area minimized any possible influence that they could have had on the results.

The procedure that was followed for the compression tests is described in detail by Steinetz, et al.¹ This procedure accurately simulates the loading conditions experienced by the seals in the flow test fixture and allows the seal preloads under those conditions to be calculated from measured quantities. Multiple load cycles were applied to the seal before the preload data point was recorded to remove most of the hysteresis and permanent set that accumulates with load cycling of the seal specimens. Most permanent set occurred within the first four load cycles.

The footprint length (nominal 1 in.) and width at the end of the fourth load cycle were used along with the measured load versus compression data to calculate the estimated preload and residual interference corresponding to a given linear crush value.¹ Residual interference is defined as the distance the seal will spring back while maintaining a load of at least one pound per inch of seal. The compression cycling procedure also accounts for both the normal and frictional loads that the seals experience in the flow fixture. This procedure has been validated for the carbon seals by comparing seal overhang measurements after a flow test to residual interference measured in the compression tests. The seal overhang data agreed to within 0.001 in. to that expected from the last cycle compression data.

Compression tests were performed on all four designs of the carbon fiber braided rope seal to determine the seal preloads corresponding to the linear seal crushes used in the flow experiments. Tests were performed at compressions of 20%, 25%, and 30% of each seal's overall diameter. Primary and repeat compression tests were performed on the Carbon-1 and Carbon-2 seals at linear compressions of 0.025, 0.031, and 0.038 in. The Carbon-3 and Carbon-4 seals were tested at compressions of 0.040, 0.050, and 0.060 in. in both primary and repeat tests.

Subscale Rocket "Char" Motor Tests

As part of the preliminary feasibility assessment of the thermal barrier seal, Thiokol Corporation performed tests using a subscale (70 lbf thrust) rocket "char" motor. In these tests a 1/8 in. diameter Carbon-1 seal sealed an intentional defect (nominal 0.003 in.) in the gap-fill material between rocket case insulation blocks to simulate solid rocket motor gap defects. Burning solid rocket propellant, the rocket fired for 11 seconds generating 900 psi pressures and 5000 °F (estimated) chamber temperatures. Hot gas flowed to the thermal barrier seal while upstream and downstream temperatures were measured in two clock positions (e.g., 0° and 90°). An outboard plenum chamber ensured flow could go through the thermal barrier seal.

Results and Discussion

Seal Characterization Results

The values for equivalent core diameter, sheath thickness, and overall seal density are presented in Table II for each type of carbon seal. Of the 1/8 in. seals, Carbon-1 had the largest core diameter at 0.064 in. and the smallest sheath thickness at 0.025 in. Carbon-2 seals had a core diameter of 0.038 in. and a sheath thickness of 0.044 in., while Carbon-2A seals had a core diameter of 0.036 in. and a sheath thickness of 0.045 in. The relative proportions of the core and sheath corresponded to the designs of these

seals. All three designs were about 1/8 in. in diameter, so Carbon-1 seals with only five sheath layers had a much larger core than Carbon-2 and Carbon-2A seals which had ten and nine sheath layers, respectively. Overall seal density was inversely related to the number of sheath layers. The seal with the most sheath layers, Carbon-2, was the least dense seal, while the seal with the fewest sheath layers, Carbon-1, had the highest density.

The two larger seal designs, Carbon-3 and Carbon-4, had comparable sheath thicknesses and core diameters. Both seals had a sheath thickness of 0.047 in., but their core diameters were slightly different at 0.107 in. for Carbon-3 and 0.100 in. for Carbon-4. These values were very similar because both designs had five sheath layers. The overall seal density for each type of seal was different, though. The Carbon-3 design was more dense than the Carbon-4 seal due to the difference in core fiber sizes. The larger core fibers in Carbon-4 seals did not pack together as closely as the smaller core fibers in Carbon-3 seals did. This created more void space in Carbon-4 seals and lowered their overall seal density.

Burn Test Results

The amount of time to burn through each type of seal is shown in Figure 5. In this figure, the number of specimens that were tested is given under the name of each seal type, and the average burn-through time is found above each bar. It is obvious from this figure that the carbon fiber braided rope seals are the most burn-resistant type of seal that was tested. The 1/8 in. diameter designs (Carbon-1, Carbon-2, and Carbon-2A) endured the 5500 °F oxyacetylene torch for about two minutes, three times as long as the next nearest seal, the phenolic fiber seal. The larger carbon seals, Carbon-3 and Carbon-4, were even more impressive, lasting about six and a half minutes in the flame. This is greater than three times the Shuttle solid rocket motor burn time of 2 minutes, 4 seconds. After the carbon seals were removed from the flame, they remained soft and flexible, even in the area that was affected by the flame, with no evidence of fiber melting. All other non-carbon seals lasted less than 15 seconds, including the 1/8 in. diameter stainless steel rod which only lasted five seconds. The conventional O-ring materials, Viton (Shuttle solid rocket motor seal material) and Buna-N, only lasted seven and five seconds, respectively. The all-ceramic seals lasted six seconds, while the hybrid seals lasted 14 seconds. All of the non-carbon seals showed signs of charring or melting after removal from the flame, and many became very brittle in the area that was burned.

Carbon-3 and Carbon-4 seals with nominal diameters of 0.20 in. lasted about six and a half minutes in the oxyacetylene torch. In comparison, 1/8 in. diameter

Carbon-1, Carbon-2, and Carbon-2A seals lasted about two minutes. Factors contributing to this threefold increase in burn resistance include an increase in seal diameter by a factor of 1.6 from 1/8 in. to 0.20 in. and an improvement in sheath braid density. Carbon-3 and Carbon-4 seals were not only larger than Carbon-1 and Carbon-2 seals, but they also had a higher braid angle of 65° (nominal) as opposed to 45° in the smaller seals. The higher braid angle combined with more braid carriers (12 and 24 carriers for Carbon-3 and Carbon-4 vs. 8 carriers for Carbon-1 and Carbon-2) created a more closely packed seal with a tighter sheath and is believed to have significantly contributed to the greater burn resistance of the larger diameter seals.

As shown in Figure 5, there was a slight difference in the burn resistance of Carbon-3 and Carbon-4 seals. Carbon-3 seals lasted an average of 387 seconds (6 minutes 27 seconds) in the flame, while Carbon-4 seals lasted an average of 399 seconds (6 minutes 39 seconds). This difference of only 12 seconds over a six to seven minute test is most likely not significant in that it is only a three percent difference in time to burn through the seals. However, it is possible that the larger diameter pitch fibers in the core of Carbon-4 seals (see Table 1) provided a very small improvement in the burn resistance of this seal design over the Carbon-3 design that had smaller PAN-based fibers in its core.

Mass-Loss Mechanism.—The mass-loss mechanism for the carbon seals is believed to be carbon oxidation. Depending on material type, carbon fibers begin to oxidize at temperatures in the range of 600 to 900 °F.^{5, 6, 7} Mass loss is not due to carbon sublimation because this process occurs at 6900 °F,¹¹ significantly above the 5500 °F flame temperature. Further evidence that the mass-loss mechanism is primarily oxidation is that when adjusting the flame from neutral (as described herein) to heavily oxidizing, burn-through times for Carbon-1 and Carbon-2 seals were only 8% of those reported in Figure 5.

Products of combustion in the solid rocket motor include liquid alumina (Al₂O₃) and gaseous CO, ClO₂, Cl, HCl, and H₂, none of which are oxidative. Hence, it is believed that the neutral flame in ambient air (oxidizing) is a conservative (i.e., more aggressive) environment for performing material screening burn tests. It is expected that oxidation rates within the rocket environment will be slower than those exhibited herein.

Flow Test Results

Flow rates for the four carbon seal designs at different levels of linear compression are summarized in Figure 6 at 60 psi and 70, 500, and 900 °F after scrubbing. Results for Carbon-1 and Carbon-2 seals are an average for two tests,

while those for Carbon-3 and Carbon-4 are for one test only. As shown by the flow results for Carbon-1 and Carbon-2 seals, flow resistance increased with higher compression levels. Figure 7 presents flow versus pressure data for the 0.20 in. diameter Carbon-3 seal at a linear compression of 0.040 in. (20%) at pressures of 2 to 100 psid and temperatures of 70, 500, and 900 °F. The flow through this seal is high enough to permit a leak check of the primary and secondary O-rings without "false-positives." Primary sealing of the nozzle joints would still be the responsibility of the O-rings, so enough flow must pass through the thermal barrier seal so as not to mistakenly qualify for use a damaged or non-working O-ring. Figure 7 is representative of the flow versus pressure curves recorded for the other carbon seals. It shows that the flow rate at each temperature was approximately a linear function of pressure. Additionally, both Figures 6 and 7 show that flow rates dropped for each seal as the temperature was increased. This phenomenon is explained by the relationship that gas viscosity increases with temperature, $\mu \propto T^{2/3}$. Thus, as the viscosity of the gas flowing past the seals increased, the flow rate decreased. This decrease in flow rate through braided rope seals as temperature increases was observed previously by Steinetz and Adams.²

Effect of Core Fiber Diameter.—Core fiber diameter also affected flow rates. As shown in Table I, the core fibers in Carbon-3 seals had a diameter of 2.76×10^{-4} in. (6.9 μm), while those in Carbon-4 seals were 4.4×10^{-4} in. (11 μm). The flow rates given in Figure 6 for Carbon-4 seals are about 20% greater than those for Carbon-3 seals. Because the larger core fibers in Carbon-4 seals did not pack together as closely as the smaller core fibers in Carbon-3 seals did, larger gaps and flow paths formed through the core of Carbon-4 seals.

Effect of Hot Scrubbing.—No major damage due to scrubbing was observed on any of the carbon seals at the conclusion of the flow tests. Any damage that was seen was concentrated immediately around the lap joints and was characterized mainly by fraying of the seal ends. Figure 8a shows a close-up view of a Carbon-1 seal tested at 0.025 in. (20%) linear compression after ten scrub cycles. Some minor damage can be observed around the lap joint. Figure 8b shows a close-up view of a Carbon-4 seal tested at 0.040 in. (20%) linear compression after 10 scrub cycles. Again, only minor damage can be seen at the lap joint. Minor fraying of the sheath fibers was rarely seen in other areas of the seal specimens.

Carbon seal flow rates typically rose after hot scrubbing during flow tests. After 500 °F testing Carbon-1 and Carbon-2 flow rates rose as much as 30%

and Carbon-3 and Carbon-4 seal flows rose less than 10%, as compared to the flow rates before scrubbing. Post-scrub room temperature flows for all seals were done after time spent at 500 °F (2 hours) and 900 °F (1.5 hours). Post-scrub room temperature flow rates for Carbon-1 and Carbon-2 doubled and those for Carbon-3 and Carbon-4 rose 80%, as compared to their pre-scrub values. It is believed that much of the seal flow rate increase is due to oxidation that occurred while the seal soaked at these high temperatures. A simple test was performed to test this hypothesis in which short lengths of carbon seal were heated in a furnace at different temperatures for two hour exposures. Seal weights were measured before and after exposure to the furnace. Results of this test showed that a weight loss of only 1% occurred after two hours at 500 °F, but a 33% weight loss occurred after two hours at 900 °F. Clearly the carbon seals oxidized when exposed to temperatures of 900 °F for extended periods of time, and the associated weight loss that took place contributed to the increased flow rates after scrubbing.

Compression Test Results

Table III summarizes the results of the compression tests performed on all four carbon seal designs. Values listed in this table include the measured contact width, preload, and residual interference for each amount of linear compression, or crush, at which the tests were performed. Figure 9 shows the load versus displacement characteristics for the 0.20 in. diameter Carbon-3 seal for a linear crush of 0.040 in. (20% linear compression). This figure is typical of the type of data that is recorded from a compression test on the carbon seals. It shows that the load versus displacement curves for each load cycle converge as the number of cycles increases.

Contact Width.—As shown in Table III the contact width increased for every seal design as the amount of linear crush was increased. This shows that the carbon seals continued to spread and flatten out as they experienced larger amounts of compression. In each test, the seal footprint pattern left on the pressure sensitive film after a compression cycle was solid and continuous. This indicates that during a flow test continuous contact is made between the walls of the flow fixture and the seal, minimizing leakage past the seal. No major differences in contact width were seen between the two 1/8 in. diameter seals, Carbon-1 and Carbon-2. However, the contact widths of the two larger seals did exhibit some differences. At 0.040 and 0.050 in. of linear compression, Carbon-3 seals had larger contact widths than Carbon-4 seals. This was probably due to the greater ability of the smaller core fibers in Carbon-3 seals to move past each other and spread out as compared to the larger core fibers in Carbon-4 seals. These differences were minimized at

0.060 in. of compression, though, as the contact widths of the two seals were almost identical. As expected, contact width increased as seal diameter increased from the 1/8 in. diameter seals to the 0.20 in. diameter seals.

Seal Preload.—The amount of seal preload also increased as the amount of linear crush increased for each type of carbon seal. Although no differences were found in the contact widths of the Carbon-1 and Carbon-2 seals, there were rather significant differences in the preloads of these two seal designs, as shown in Table III. For each compression level, the preload for Carbon-1 seals was larger than for Carbon-2 seals, and the difference between the two designs increased as the amount of linear crush increased. Thus, Carbon-1 seals were stiffer than Carbon-2 seals. The reason for this difference is believed to be related to the architecture of the two seals as shown in Table I. Carbon-2 seals had ten sheath layers and a much smaller core area than Carbon-1 seals which only had five sheath layers. In a tightly-packed core of uniaxial fibers, there is little room for individual fibers to move with respect to one another when they are compressed. In contrast, fibers in the sheath are oriented at an angle with each other and are better able to slide past each other when the seal is compressed. Thus, because Carbon-2 seals had a larger percentage of their total volume in the sheath as compared to Carbon-1 seals, the Carbon-2 design was more easily compressed and had lower preload values.

Carbon-3 and Carbon-4 seals did not exhibit the same type of behavior in terms of preload as the smaller seals did. Carbon-4 seals were stiffer at the lowest crush level (0.040 in.), while Carbon-3 seals were stiffer at the highest crush level (0.060 in.). Both seals had the same preload at 0.050 in. of linear compression. The differences in preload behavior is again probably related to the difference in core fibers between the seals. These larger seal designs were generally stiffer than Carbon-2 seals but were still not as stiff as Carbon-1 seals.

Residual Interference.—As with the contact width and preload, the residual interference also increased for each type of seal as percent linear crush increased. Carbon-2 seals consistently had higher residual interference values at each level of linear crush than Carbon-1 seals had. Because Carbon-1 seals were stiffer than Carbon-2 seals, the higher preloads on the Carbon-1 seals caused them to experience larger amounts of permanent set and to lose resilience. Thus, Carbon-1 seals had less "springback" in them which led to lower residual interference values. For the larger seal designs, the residual interference of Carbon-3 and Carbon-4 seals was almost identical for each amount of linear compression. Residual interference for Carbon-3 and Carbon-4 seals was 0.019 in. even for the

lowest compression (20%) and meets the design requirement to follow nozzle joint movement/separation (0.003-0.005 in.) during Shuttle solid rocket motor operation. Table III also shows that residual interference scaled approximately with seal diameter. When seal diameter was increased by a factor of 1.6 from 0.125 in. to 0.200 in., residual interference was also increased by that ratio for each level of percent compression.

Results of Preliminary Thiokol Char Motor Tests on Carbon Seals

A length of Carbon-1 seal was tested by Thiokol in a subscale rocket motor to verify that it would withstand the Shuttle solid rocket motor environment. The subscale motor, or "char" motor, simulates the thermal conditions of the full scale motor's environment by burning solid rocket propellant at corresponding chamber pressure conditions. Blocks of phenolic insulation surrounding the chamber in the char motor were modified so that a 12 in. diameter Carbon-1 seal could be placed in the gap between the blocks, as shown in Figure 10a. The seal was compressed from its original 0.125 in. diameter down to 0.094 in., and the portion of the seal that faced the hot side of the chamber was exposed to an intentional 0.003 in. circumferential joint defect. Temperatures and pressures were measured on both the hot side and cold side of the seal during testing.

Throughout the test duration of approximately 11 sec, a significant drop in temperature was measured across the seal. Figure 10b shows that the maximum temperature seen on the hot side of the seal was about 2500 °F, while the cold side temperature was around 110 °F, for a 2400 °F temperature drop across the 1/8 in. diameter seal. Pressure readings indicated that there was gas flow across the seal. Just as importantly, there was no apparent burning or charring of the carbon seal after removal from the motor.

Summary and Conclusions

The 5500 °F combustion gases in the Shuttle solid rocket motors are kept a safe distance away from the seals in assembly joints by thick layers of phenolic insulation and by special compounds that fill assembly split-lines in this insulation. Parasitic leakage paths have occasionally opened up in the gap-filling compounds and allowed a direct flowpath of hot gases to the seals causing O-ring seal erosion and charring. NASA and solid rocket motor manufacturer Thiokol are investigating the feasibility of using NASA braided thermal barrier seals upstream of the primary O-rings. These thermal barrier seals would resist the hot gases and prevent them from reaching the primary O-rings.

The thermal resistance of different material systems was assessed by exposing seals to an oxyacetylene torch at 5500 °F (representative of solid rocket motor combustion temperatures) and measuring time for burn through. Seals braided out of carbon fibers exhibited the longest time for burn through. Flow and durability tests were conducted on the carbon seals to examine their leakage characteristics and durability at ambient and high temperatures. Room temperature compression tests were performed to determine load versus linear compression, preload, contact area, and residual interference/resiliency characteristics. Subscale rocket "char" motor tests were performed in which hot combustion gases were allowed to flow to the thermal barrier seal to assess its thermal resistance in a rocket environment. Based on the results of these tests, the following conclusions are made:

1. The Carbon-3 and Carbon-4 seal springback of 0.019 in. is greater than the 0.003-0.005 in. joint movement/separation anticipated during rocket motor operation, providing adequate seal resiliency.

2. Carbon-3 and Carbon-4 seals resisted the oxyacetylene flame (5500 °F) for over six minutes before burn through, greater than three times Shuttle solid rocket motor burn time.

3. Subscale rocket "char" motor tests demonstrated that the thermal barrier seal resisted hot gases that flowed to the seal through an intentional gap defect. Though temperatures over 2500 °F were measured on the seal hot side, temperatures on the seal cold side were just over 100 °F during the 11 sec. rocket firing, well within the Viton nozzle O-ring temperature limits.

4. Laboratory flow, compression, burn tests, and subscale rocket "char" motor tests demonstrate the thermal barrier seal's preliminary feasibility, qualifying the seal for comprehensive test and evaluation.

References

- ¹Steinetz, B.M., Adams, M.L., Bartolotta, P.A., Darolia, R., and Olsen, A., "High Temperature Braided Rope Seals for Static Sealing Applications," NASA TM-107233 rev., July 1996 and *J. of Propulsion and Power*, Vol. 13, No. 5, 1997, pp. 675-682.
- ²Steinetz, B.M., and Adams, M.L., "Effects of Compression, Staging, and Braid Angle on Braided Rope Seal Performance," NASA TM-107504, July 1997.
- ³Thiokol report TWR-73191, "RSRM-45A Nozzle Joint No. 3 O-ring Erosion Investigation Team Final Report," October 28, 1996.
- ⁴Shemet, V., Pomytkin, A.P., and Neshpor, V.S., "High-Temperature Oxidation Behaviour of Carbon Materials in Air," *Carbon*, Vol. 31, No. 1, pp. 1-6, 1993.

⁵Bahl, O.P. and Dhama, T.L., "Oxidation Resistance of Carbon Fibers," High Temperatures-High Pressures, Vol. 19, pp. 211-214, 1987.

⁶Eckstein, B.H. and Barr, J.B., "An Accelerated Oxidation Test for Oxidation Resistant Carbon Fibers," Materials-Processes: The Intercept Point; Proceedings of the Twentieth International SAMPE Technical Conference, Minneapolis, MN, Sept. 27-29, 1988. Covina, CA, Society for the Advancement of Materials and Process Engineering, 1988, pp. 379-391.

⁷Eckstein, B.H., "The Weight Loss of Carbon Fibers in Circulating Air," 18th International SAMPE Technical Conference, October 7-9, 1986, pp. 149-160.

⁸Ballis, W., ASM Handbook, Volume 6: Welding, Brazing, and Soldering, ASM International, 1993, pp. 281-290.

⁹Udin, Funk, and Wulff, Welding for Engineers, John Wiley and Sons, Inc., 1954, pp. 211-218.

¹⁰Thornel T-300 carbon fiber Product Information, Amoco Performance Products, Inc.

¹¹Lide and Kehiaian, CRC Handbook of Thermophysical and Thermochemical Data, CRC Press, 1994, pp. 25-31.

TABLE I - BRAIDED ROPE SEAL CONSTRUCTION MATRIX

| Seal Type | Size Diameter (in) | Core | | | | Sheath | | | | | | |
|-------------|--------------------------|-----------------------------------|--------------|------------------------------------|--------------------|----------------------------------|--------|------------------------------------|---------------------|------------------------------------|----------------------------------|-----------------------------|
| | | Material | Denier | Fiber Diam (in) ^a | Number of yarns | Material | Denier | Fiber Diam (in) ^a | Number of layers | Number of carriers per layer | Number of yarns per bundle | Braid Angle (degrees) |
| Carbon | | | | | | | | | | | | |
| Carbon-1 | 0.114 | Grafil ^b 34-700 12K | 7200 | 2.76x10 ⁻⁴ | 4 | Thornel ^c T-300 1K | 600 | 2.8x10 ⁻⁴ | 5 | 8 | 1 | 45 |
| Carbon-2 | 0.125 | Grafil 34-700 12K 34-700 3K | 7200 1800 | 2.76x10 ⁻⁴ | 1 1 | Thornel T-300 1K | 600 | 2.8x10 ⁻⁴ | 10 | 8 | 1 | 45 |
| Carbon-2A | 0.125 | Grafil 34-700 12K 34-700 3K | 7200 1800 | 2.76x10 ⁻⁴ | 1 1 | Thornel T-300 1K | 600 | 2.8x10 ⁻⁴ | 9 | 8 | 1 | 45 |
| Carbon-3 | 0.200 | Grafil 34-700 12K | 7200 | 2.76x10 ⁻⁴ | 10 | Thornel T-300 1K | 600 | 2.8x10 ⁻⁴ | 5 | 12,12, 24,24,24 | 1 | 65 in 1st 60 in 5th |
| Carbon-4 | 0.194 | Amoco ^d P25 2K | 2900 | 4.4x10 ⁻⁴ | 21 | Thornel T-300 1K | 600 | 2.8x10 ⁻⁴ | 5 | 12,12, 24,24,24 | 1 | 65 in 1st 60 in 5th |
| Phenolic | | | | | | | | | | | | |
| Phenolic-1 | 0.125 | Kynol ^e KPY-0204-1 | 4500 | 6.0x10 ⁻⁴ | 4 | Kynol KY-02 | 1100 | 6.0x10 ⁻⁴ | 4 | 8 | 1 | 45 |
| Hybrid | | | | | | | | | | | | |
| NTWHY-4 | 0.120 | NX 550 ^f | 700 | 3.2x10 ⁻⁴ | 154 | HS 188 ^g | 110 | 1.6x10 ⁻³ | 1 | 24 | 6 | 65 |
| All-Ceramic | | | | | | | | | | | | |
| NTWAC-2 | 0.120 | NX 550 | 700 | 3.2x10 ⁻⁴ | 109 | NX 550 | 700 | 3.2x10 ⁻⁴ | 2 | 8 | 1 | 56 |

Notes:

^a1x10⁻³ in = 25 μm

^bGrafil type 34-700 carbon fibers, Grafil Inc. product

^cThornel T-300 carbon fibers, Amoco Performance Products, Inc. product

^dAmoco P25 pitch fibers, Amoco Performance Products, Inc. product

^eKynol fibers, American Kynol, Inc. product, 76% C, 18% O, 6% H

^fNX 550 = Nextel 550 fiber, 3M product, 73% Al₂O₃, 27% SiO₂

^gHS 188 = Haynes 188 wire, Fort Wayne Metals product, 38% Co, 22% Ni, 22% Cr, 14% W, 3% Fe, 1.25% Mn, 0.5% Si, 0.08% La, 0.015% B, 0.05% C

TABLE II - EQUIVALENT CORE DIAMETER, SHEATH THICKNESS, AND OVERALL SEAL DENSITY CALCULATIONS

| Seal Type | Number of Sheath Layers | Diameter (in) | Equivalent Core Diameter (in) | Sheath Thickness (in) | Overall Seal Density (g/cc) |
|-----------|-------------------------|---------------|-------------------------------|-----------------------|-----------------------------|
| Carbon-1 | 5 | 0.114 | 0.064 | 0.025 | 1.099 |
| Carbon-2 | 10 | 0.125 | 0.038 | 0.044 | 0.998 |
| Carbon-2A | 9 | 0.125 | 0.036 | 0.045 | 1.019 |
| Carbon-3 | 5 | 0.200 | 0.107 | 0.047 | 1.035 |
| Carbon-4 | 5 | 0.194 | 0.100 | 0.047 | 1.018 |

TABLE III - CARBON FIBER BRAIDED ROPE SEAL CONTACT WIDTH, PRELOAD, AND RESIDUAL INTERFERENCE FOR SEVERAL LINEAR CRUSH CONDITIONS

| Seal Type | Diameter (in) | Nom. Percent Linear Crush (%) | Linear Crush (in) | Number of Sheath Layers | Contact Width (in) | Preload (psi) | Residual Interference ^a (in) |
|-----------|---------------|-------------------------------|-------------------|-------------------------|--------------------|---------------|---|
| Carbon-1 | 0.114 | 20 | 0.025 | 5 | 0.038 | 430 | 0.012 |
| | | 25 | 0.031 | | 0.052 | 770 | 0.015 |
| | | 30 | 0.038 | | 0.062 | 1300 | 0.019 |
| Carbon-2 | 0.125 | 20 | 0.025 | 10 | 0.039 | 380 | 0.013 |
| | | 25 | 0.031 | | 0.055 | 465 | 0.019 |
| | | 30 | 0.038 | | 0.065 | 740 | 0.023 |
| Carbon-3 | 0.200 | 20 | 0.040 | 5 | 0.063 | 310 | 0.019 |
| | | 25 | 0.050 | | 0.082 | 490 | 0.027 |
| | | 30 | 0.060 | | 0.099 | 930 | 0.033 |
| Carbon-4 | 0.194 | 20 | 0.040 | 5 | 0.052 | 430 | 0.019 |
| | | 25 | 0.050 | | 0.077 | 490 | 0.028 |
| | | 30 | 0.060 | | 0.100 | 800 | 0.035 |

^aResidual interference is defined as the distance that the seal will spring back while maintaining a load of at least 1 pound per inch of seal.

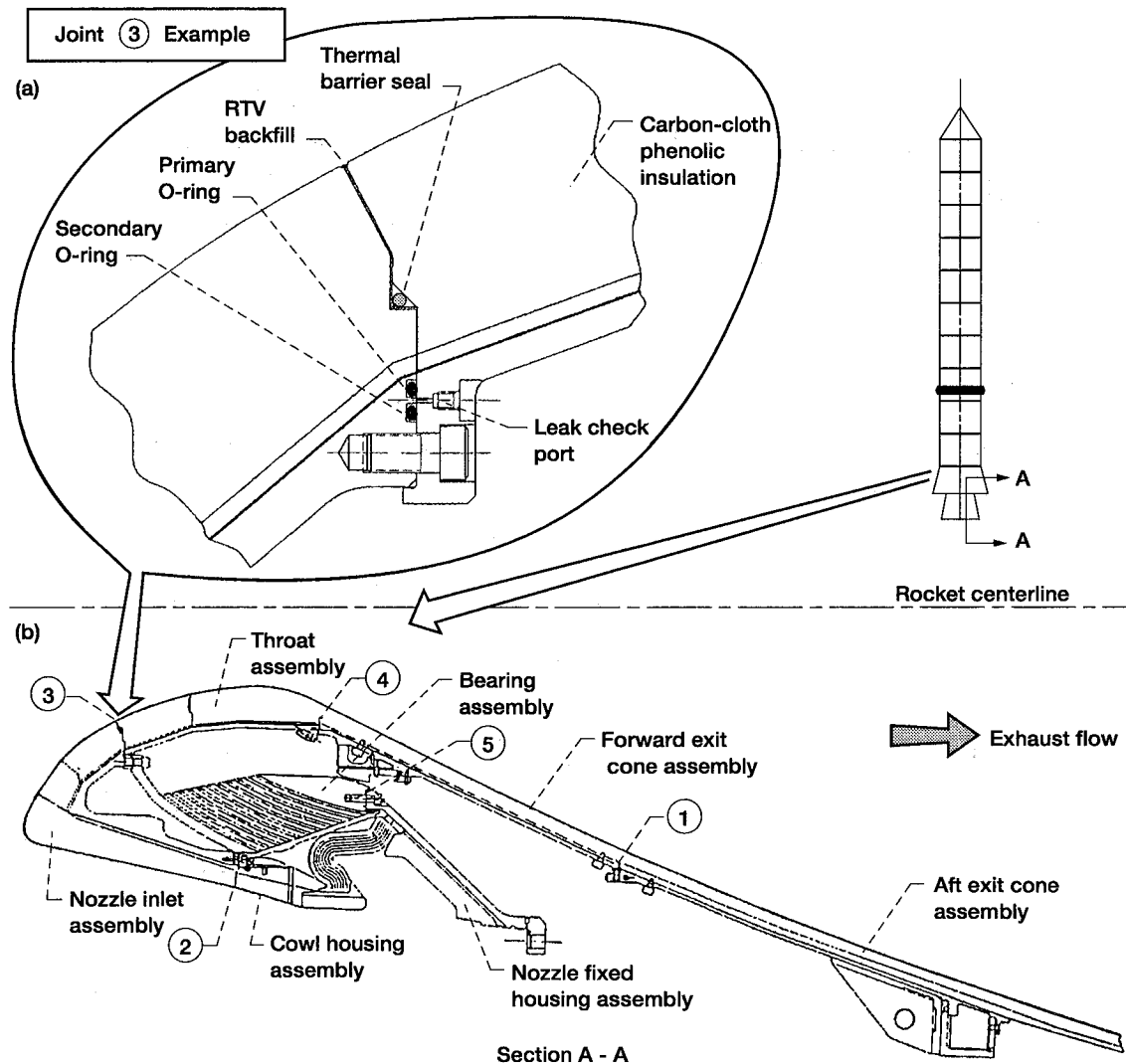


Figure 1.—Potential Shuttle solid rocket motor joint locations for candidate thermal barrier seal. (a) Enlarged view of Joint 3 showing primary and secondary pressure O-rings, leak-check port, and proposed thermal barrier seal location. (b) Overall nozzle cross-section (half view).

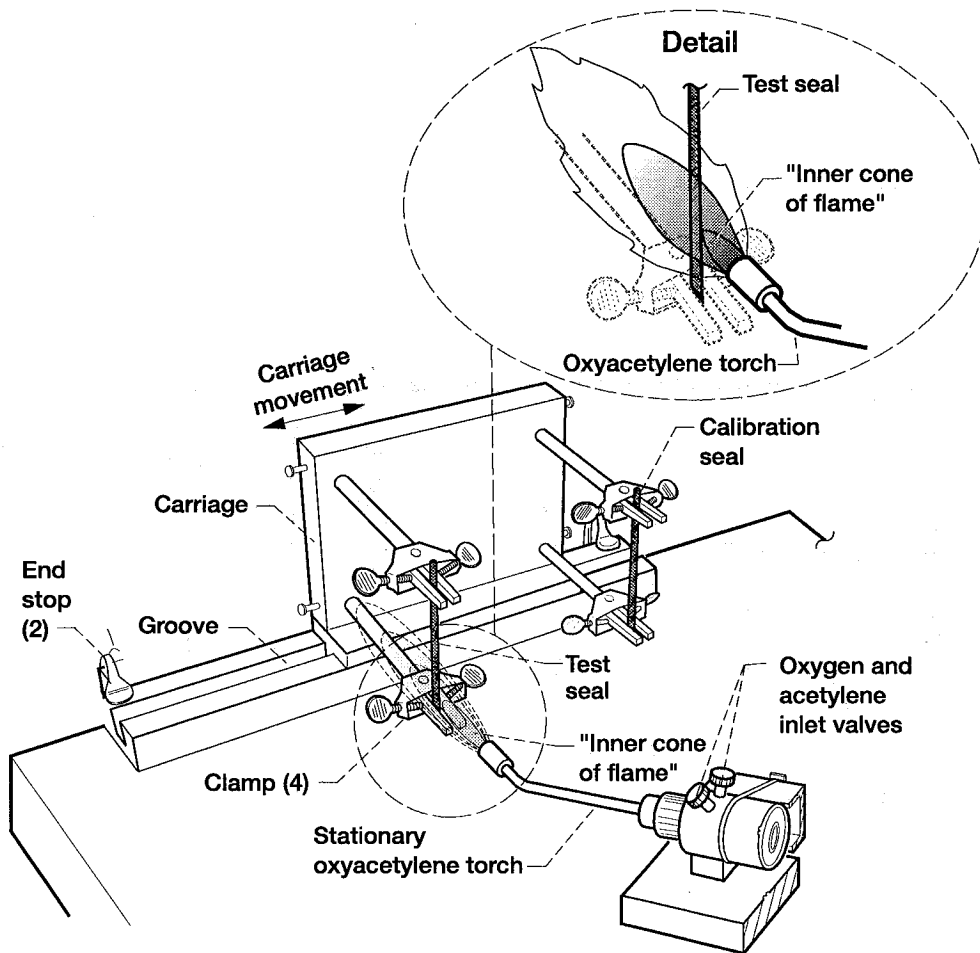


Figure 2.—Schematic of burn test fixture.

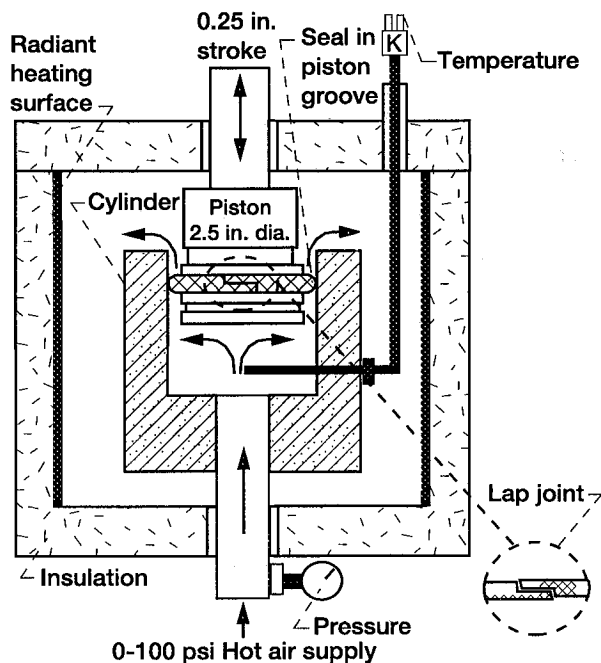


Figure 3.—Schematic of flow fixture.

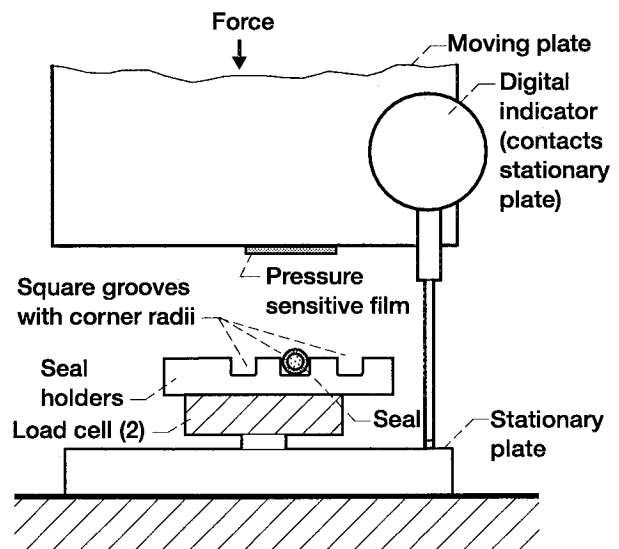


Figure 4.—Schematic of compression fixture.

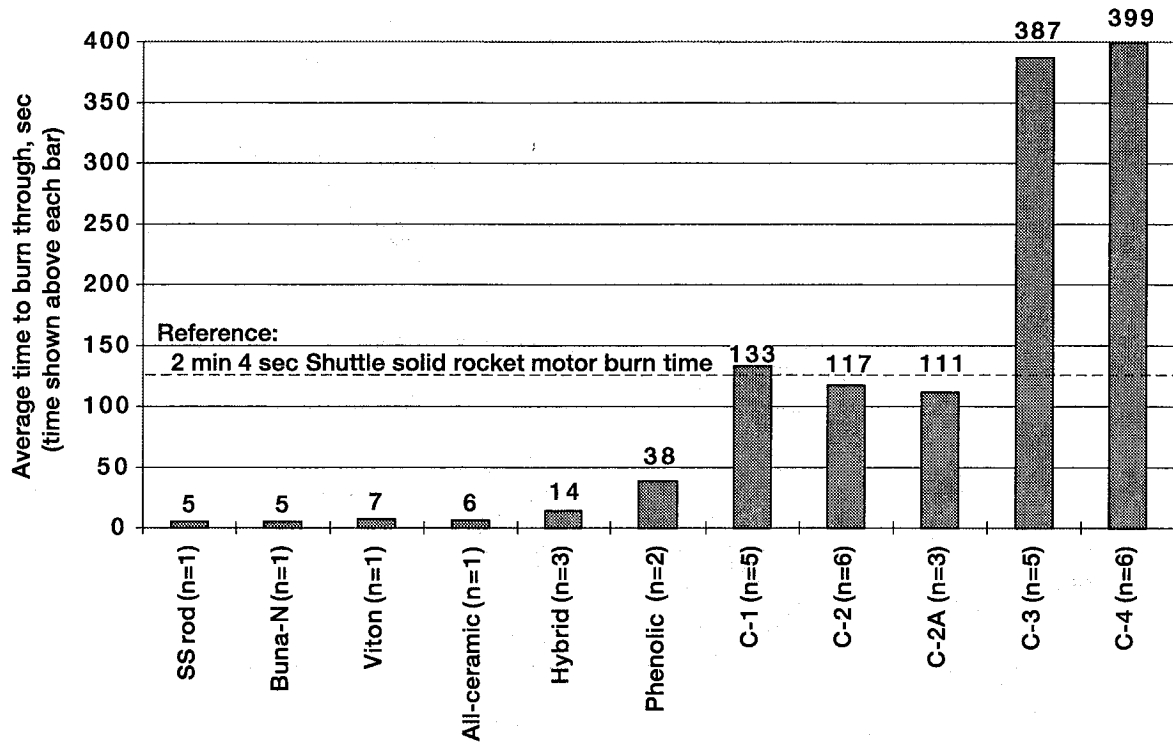


Figure 5.—Oxyacetylene torch burn test results (n = number of tests performed).

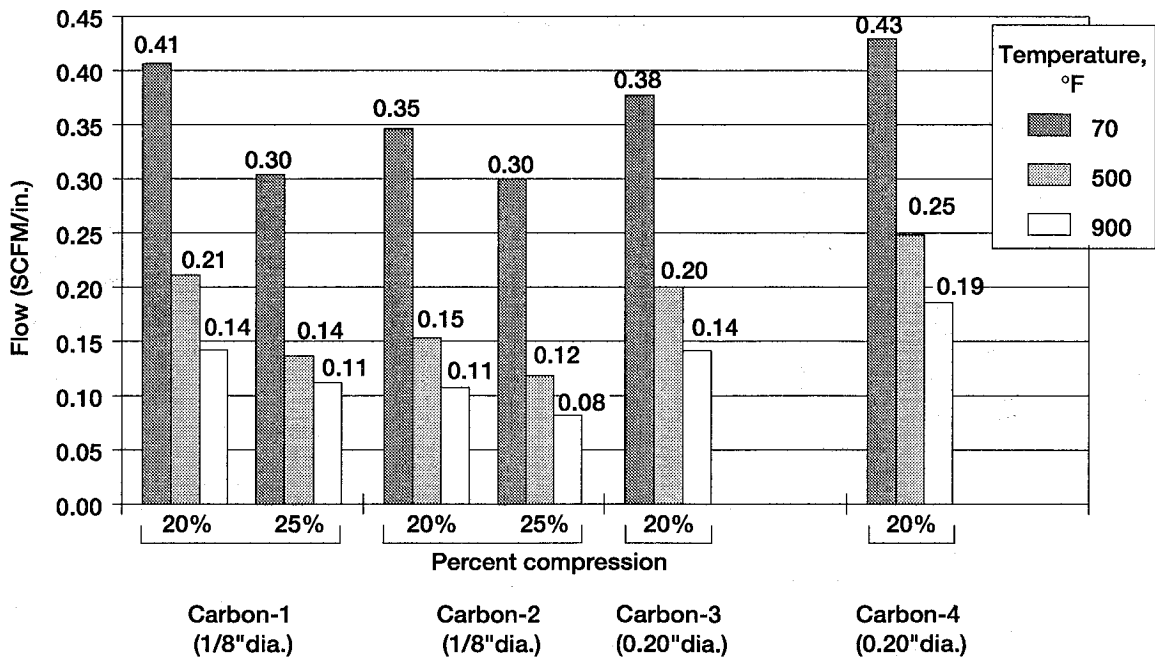


Figure 6.—The effect of temperature, seal type, and compression on seal flow after scrubbing, $\Delta P = 60$ psi.

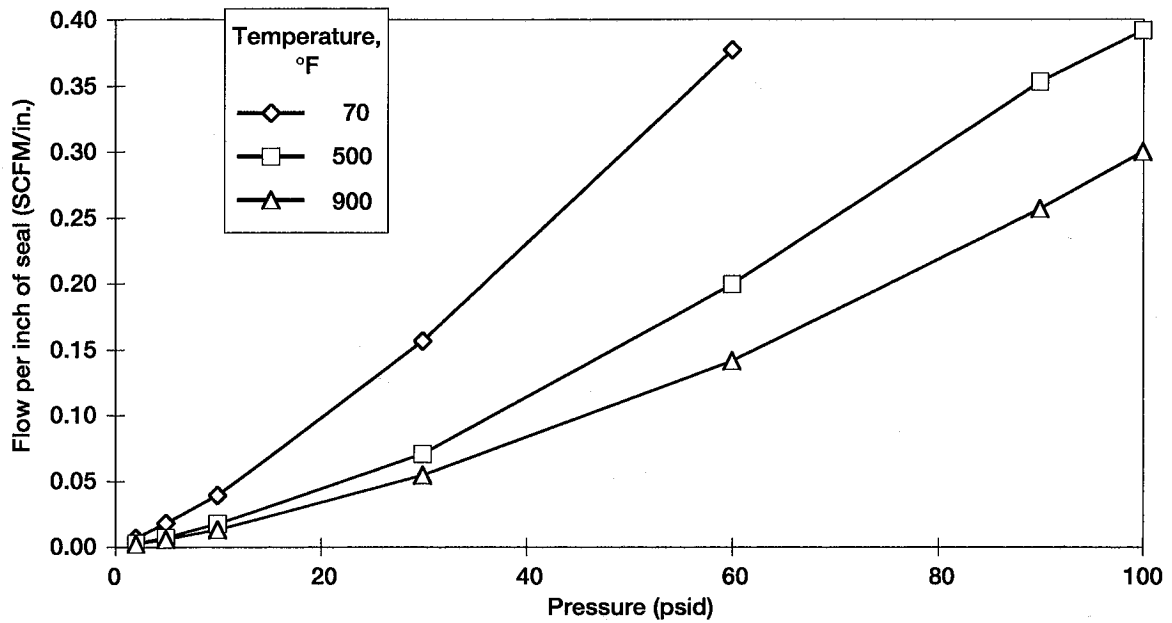


Figure 7.—Flow vs. pressure data for three temperatures, 0.20 in. diameter Carbon-3, 0.04 in. (20%) linear compression, after scrubbing.

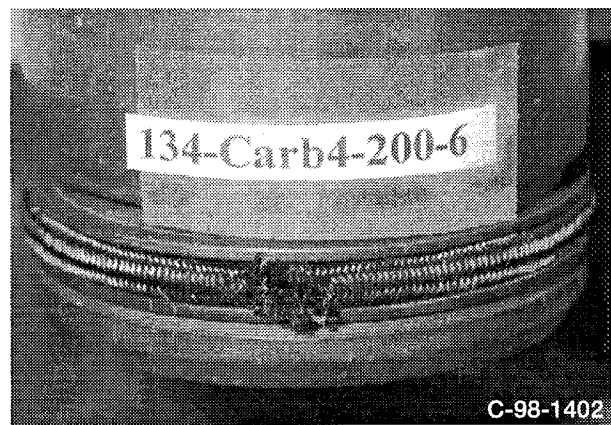
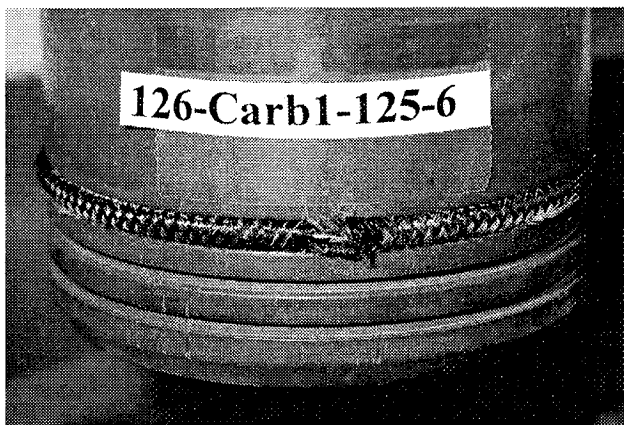


Figure 8.—Photos of carbon seals after 900 °F flow/scrubbing tests. (a) Carbon-1 (1/8 in. diameter). (b) Carbon-4 (0.20 in. diameter).

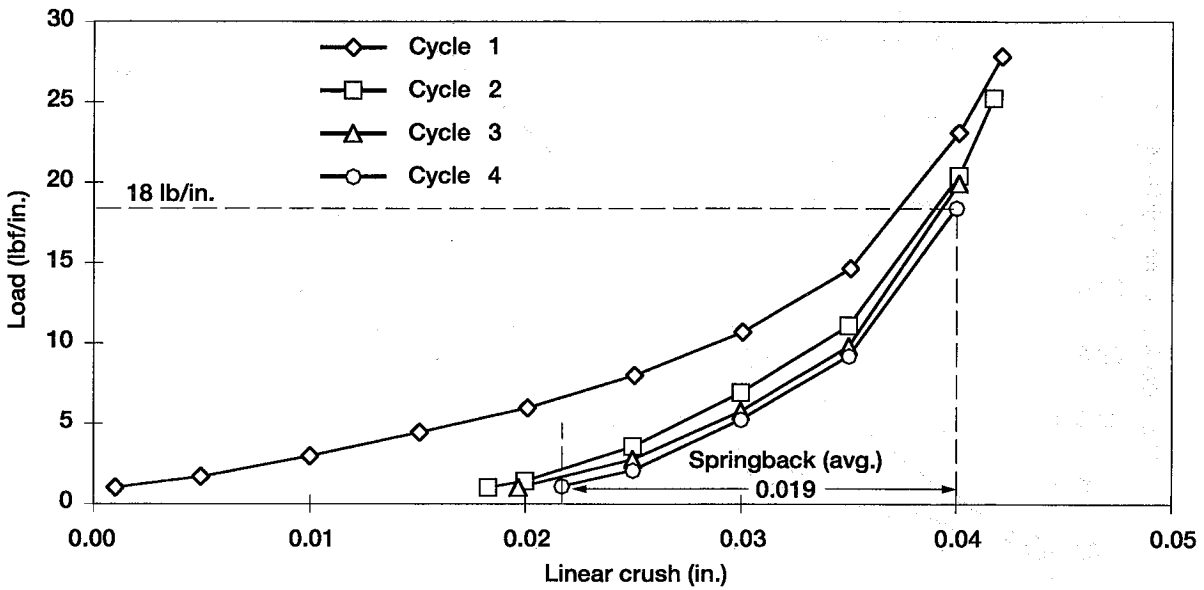


Figure 9.—Load vs. linear compression data for four cycles, 0.20 in. diameter Carbon-3 seal at representative compression of 0.04 in. (20%).

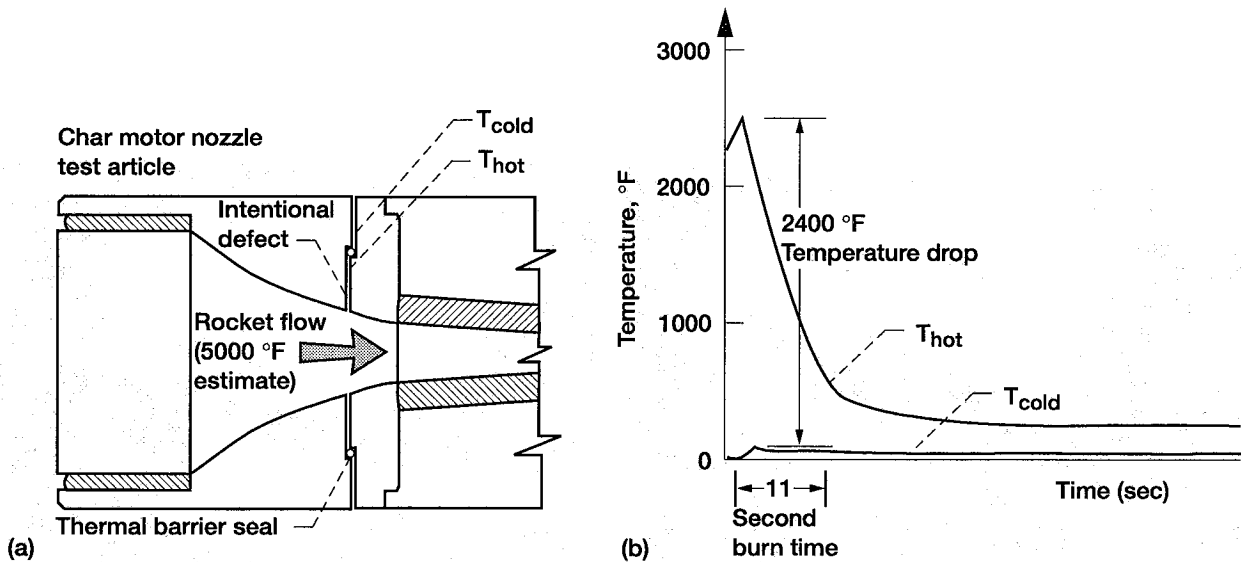


Figure 10.—Preliminary subscale (70 lbf thrust) "char" motor tests examining thermal barrier seal (Carbon-1) effectiveness. (a) Test configuration: Carbon-1 seal seals intentional joint defect. (b) Temperature data: Upstream (T_{hot}) and downstream (T_{cold}) sides of seal. (Courtesy of Thiokol Corp.)

REPORT DOCUMENTATION PAGE

Form Approved
OMB No. 0704-0188

Public reporting burden for this collection of information is estimated to average 1 hour per response, including the time for reviewing instructions, searching existing data sources, gathering and maintaining the data needed, and completing and reviewing the collection of information. Send comments regarding this burden estimate or any other aspect of this collection of information, including suggestions for reducing this burden, to Washington Headquarters Services, Directorate for Information Operations and Reports, 1215 Jefferson Davis Highway, Suite 1204, Arlington, VA 22202-4302, and to the Office of Management and Budget, Paperwork Reduction Project (0704-0188), Washington, DC 20503.

| | | | | |
|--|---|--|--|--|
| 1. AGENCY USE ONLY (Leave blank) | | 2. REPORT DATE July 1998 | 3. REPORT TYPE AND DATES COVERED Technical Memorandum | |
| 4. TITLE AND SUBTITLE Feasibility Assessment of Thermal Barrier Seals for Extreme Transient Temperatures | | | 5. FUNDING NUMBERS WU-523-53-13-00 | |
| 6. AUTHOR(S) Bruce M. Steinetz and Patrick H. Dunlap, Jr. | | | | |
| 7. PERFORMING ORGANIZATION NAME(S) AND ADDRESS(ES) National Aeronautics and Space Administration Lewis Research Center Cleveland, Ohio 44135-3191 | | | 8. PERFORMING ORGANIZATION REPORT NUMBER E-11196 | |
| 9. SPONSORING/MONITORING AGENCY NAME(S) AND ADDRESS(ES) National Aeronautics and Space Administration Washington, DC 20546-0001 | | | 10. SPONSORING/MONITORING AGENCY REPORT NUMBER NASA TM-1998-208484 AIAA-98-3288 | |
| 11. SUPPLEMENTARY NOTES Prepared for the 34th Joint Propulsion Conference cosponsored by AIAA, ASME, SAE, and ASEE, Cleveland, Ohio, July 12-15, 1998. Bruce M. Steinetz, NASA Lewis Research Center and Patrick H. Dunlap, Jr., Modern Technologies Corporation, 7530 Lucerne Drive, Islander Two, Suite 206, Middleburg Heights, Ohio 44130. Responsible person, Bruce Steinetz, organization code 5950, (216) 433-3302. | | | | |
| 12a. DISTRIBUTION/AVAILABILITY STATEMENT Unclassified - Unlimited Subject Category: 37 This publication is available from the NASA Center for AeroSpace Information, (301) 621-0390. | | | 12b. DISTRIBUTION CODE Distribution: Nonstandard | |
| 13. ABSTRACT (Maximum 200 words) The assembly joints of modern solid rocket motor cases are generally sealed using conventional O-ring type seals. The 5500+ °F combustion gases produced by rocket motors are kept a safe distance away from the seals by thick layers of phenolic insulation. Special compounds are used to fill insulation gaps leading up to the seals to prevent a direct flowpath to them. Design criteria require that the seals should not experience torching or charring during operation, or their sealing ability would be compromised. On limited occasions, NASA has observed charring of the primary O-rings of the Space Shuttle solid rocket nozzle assembly joints due to parasitic leakage paths opening up in the gap-fill compounds during rocket operation. NASA is investigating different approaches for preventing torching or charring of the primary O-rings. One approach is to implement a braided rope seal upstream of the primary O-ring to serve as a thermal barrier that prevents the hot gases from impinging on the O-ring seals. This paper presents flow, resiliency, and thermal resistance for several types of NASA rope seals braided out of carbon fibers. Burn tests were performed to determine the time to burn through each of the seals when exposed to the flame of an oxyacetylene torch (5500 °F), representative of the 5500 °F solid rocket motor combustion temperatures. Rope seals braided out of carbon fibers endured the flame for over six minutes, three times longer than solid rocket motor burn time. Room and high temperature flow tests are presented for the carbon seals for different amounts of linear compression. Room temperature compression tests were performed to assess seal resiliency and unit preloads as a function of compression. The thermal barrier seal was tested in a subscale "char" motor test in which the seal sealed an intentional defect in the gap insulation. Temperature measurements indicated that the seal blocked 2500 °F combustion gases on the upstream side with very little temperature rise on the downstream side. | | | | |
| 14. SUBJECT TERMS Seals; Space Shuttle; Solid rocket motor; Fluid flow; Design; Test; Carbon; Braid | | | 15. NUMBER OF PAGES 21 | |
| | | | 16. PRICE CODE A03 | |
| 17. SECURITY CLASSIFICATION OF REPORT Unclassified | 18. SECURITY CLASSIFICATION OF THIS PAGE Unclassified | 19. SECURITY CLASSIFICATION OF ABSTRACT Unclassified | 20. LIMITATION OF ABSTRACT | |